

Electronic Structure and Optical Properties of Nitrogen Doped SnO₂ — Simulation by DFT Method

M. MALEKI*

Department of Physics, Faculty of Science, Fouman and Shaft Branch,
Islamic Azad University, P.O. Box 43518-35875, Fouman, Iran

In this paper, nanostructured tin oxide doped with Nitrogen was investigated by first principle calculations. At first, band structure, density of states, and projected density of states were evaluated for pure tin oxide. Then, the effect of doping with Nitrogen was studied for cases when N replaces O atom, Sn atom, respectively, and in two interstitials situation. Results were compared with pure reference case. Except of one interstitial case, Nitrogen doping usually plays the role of a *p*-type doping, however the decrease of band gap occurs in all cases.

DOI: [10.12693/APhysPolA.137.272](https://doi.org/10.12693/APhysPolA.137.272)

PACS/topics: nitrogen, Tin oxide, SIESTA code, DFT, Doping

1. Introduction

Transparent conducting oxides (TCOs) are solid-state oxides that have the properties of electrical conductivity and optical transparency simultaneously [1]. SnO₂ as an oxide semiconductor has applications in many fields, such as gas sensors, solar cells, catalysis [2], etc. Pure SnO₂ is an intrinsic *n*-type material because of native oxygen vacancy defects. Various elements as a *p*-type or *n*-type dopant have been examined by different simulation methods [3–6]. Recently, there is an increasing interest in the research of nitrogen doped tin oxide for its influence on enhancement of photo catalysis or solar energy conversion effectiveness [7–8]. One should note, that atoms from group-V have one less valence electron than O, and one more valence electron than Sn. In fact, they are expected to show amphoteric behavior in SnO₂. They may act as acceptors when substituting on the O site, or as donors if incorporated on the Sn site [9]. Nitrogen as a *p*-type doping is an excellent candidate because of its high solubility and non-toxicity [8,10–12]. Nitrogen doping is also important due to its effects on absorption properties of tin oxide by narrowing of band gap or by inserting new energy states into the gap. The theoretical methods such as density functional theory (DFT) offer a reliable and an economic way for predicting different properties of a large variety of semiconductors. Also, an achievable software SIESTA code is a reasonable and efficient tool for investigating doping elements in the different structures before beginning experimental procedure [12]. In the mentioned articles it was reported that achieving *p*-type in tin oxide is more probable by nitrogen doping. Therefore, we decide to investigate the effect of nitrogen doping on tin oxide by SIESTA code but using a DFT method for simulating. Our aim was to study the effect of doping in different positions in the lattice.

2. Material and method

The following calculations are based on the fully self-consistent pseudopotential DFT method. Ab initio calculations with the local density approximation (LDA) are accomplished according to the Ceperley Alder (CA) parametrization along with double-zeta basis set with polarization functions (DZP). Norm conserving pseudo potentials that was carried out in the SIESTA code [13] were applied. We used a double zeta basis function with polarization orbitals, a confining energy shift of 250 meV, and a mesh cutoff energy of 700 Ry for the grid integration. The Brillouin zone was sampled by using a Monkhorst-Pack scheme with $(5 \times 5 \times 8)$ *k*-point sampling. The optimized 48 atoms SnO₂ supercell was made. To consider the type of substitutional defect two models were introduced. Namely, (i) a lattice atom Sn is substituted by a N atom (N_{Sn}), and (ii) a lattice atom O is substituted by a N atom (N_O). To consider the type of interstitial defect of N two other models were made (N_{in}). The location of Nitrogen in model N_{in} is marked by 1 and 2. The site 1 is located at the center of the Sn-O bond and the site 2 corresponds to the center of the two neighboring O atoms.

3. Results and discussion

The diagram of total energy versus the cutoff energy has been shown in Fig. 1. For the rutile-phase SnO₂, if the cutoff energy is fixed at 700 eV for *k*-point of $3 \times 3 \times 4$, the convergence in total energy is good. According to Fig. 2, if the *k*-point set mesh is fixed at $5 \times 5 \times 8$, the change in total energy is less than 1 meV when the cutoff. For this reason further rutile-phase SnO₂ calculation has been done for the cutoff energy value of 700 eV and the *k*-point set $5 \times 5 \times 8$.

Formation energies E_{form} for the four different N-doped models were studied to investigate the stability of different N-doped structures. The formation energies can be defined as follows [14]:

*corresponding author; e-mail: m.maleki@fshiau.ac.ir

$$E_{\text{form}} = E(\text{Sn}_{16}\text{O}_{31}\text{N}) - E(\text{Sn}_{16}\text{O}_{32}) + E(\text{O}) - E(\text{N})$$

for the substitutional N to O model,

$$E_{\text{form}} = E(\text{Sn}_{15}\text{O}_{32}\text{N}) - E(\text{Sn}_{16}\text{O}_{32}) + E(\text{Sn}) - E(\text{N})$$

for substitutional N to Sn model, and

$$E_{\text{form}} = E(\text{Sn}_{16}\text{O}_{32}\text{N}) - E(\text{Sn}_{16}\text{O}_{32}) - E(\text{N})$$

for the interstitial N-doped models. Terms $E(\text{Sn}_{16}\text{O}_{31}\text{N})$, $E(\text{Sn}_{15}\text{O}_{32}\text{N})$, $E(\text{Sn}_{16}\text{O}_{32}\text{N})$, and $E(\text{Sn}_{16}\text{O}_{32})$ indicate the total energy of the supercell with and without N, respectively. The energy of the one Sn atom in the bulk is $E(\text{Sn})$. Other energies, i.e., $E(\text{N})$ and $E(\text{O})$ are determined by the energy of an N atom in N₂, and of an O atom in an O₂ molecule, respectively, using formulas $E(\text{N}) = \frac{1}{2}E(\text{N}_2)$, $E(\text{O}) = \frac{1}{2}E(\text{O}_2)$.

According to our calculation the formation energies of N_{Sn}, N_O, N_{in-1} and N_{in-2} are 4.26 eV, 1.29 eV, -9.31 eV, and -7.58 eV, respectively. The calculations show that the doping of N at the O site has the lowest formation energy (1.29 eV). This behavior can easily be understood in terms of the atomic sizes of the O and N atoms. The atomic radii of O and N are 6 and 6.5 Å, respectively. Due to the radius similarity, N at the O site will not distort the structure and it is therefore expected that the O site will be favorable for N doping. Although N at the interstitial site 1 has the lowest formation energy among the four dopant sites, it is not important from the magnetism point of view. The total energies calculated for N_{in-1} and N_{in-2} are, respectively, -15662 eV and -15660 eV. Apparently, N_{in-1} structure has the lowest total energy what indicates that it is the most energetically favored structure among two interstitial states [15].

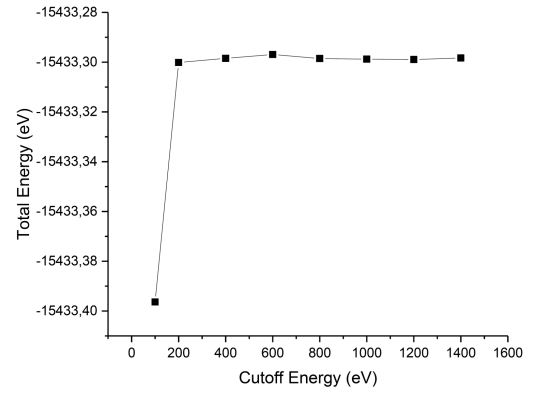


Fig. 1. Diagram of Total Energy versus to Cutoff Energy for pure tin oxide.

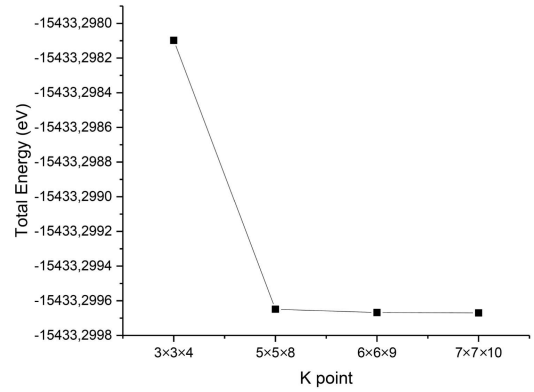


Fig. 2. Diagram of Total Energy versus the K point mesh for the cutoff energy 700 eV.

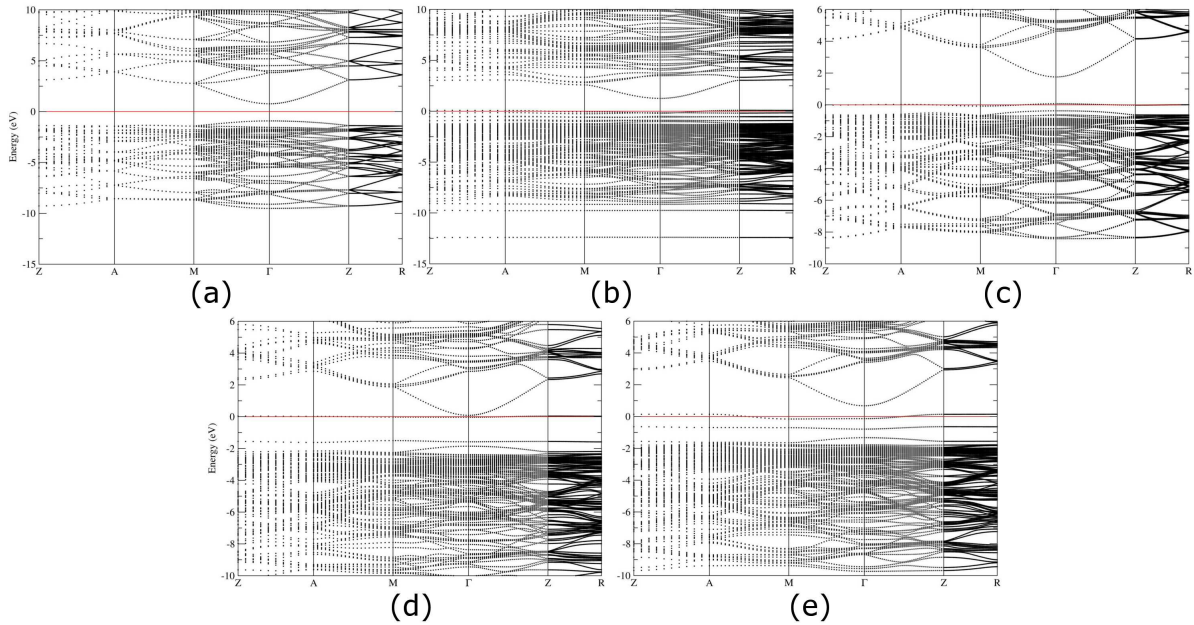


Fig. 3. The band structure of pure tin oxide and nitrogen doped tin oxide. (a) pure SnO₂, (b) NSnO₂ — N instead of Sn, (c) NSnO₂ — N instead of O, (d) NSnO₂ — N-in-1, (e) NSnO₂ — N-in-2.

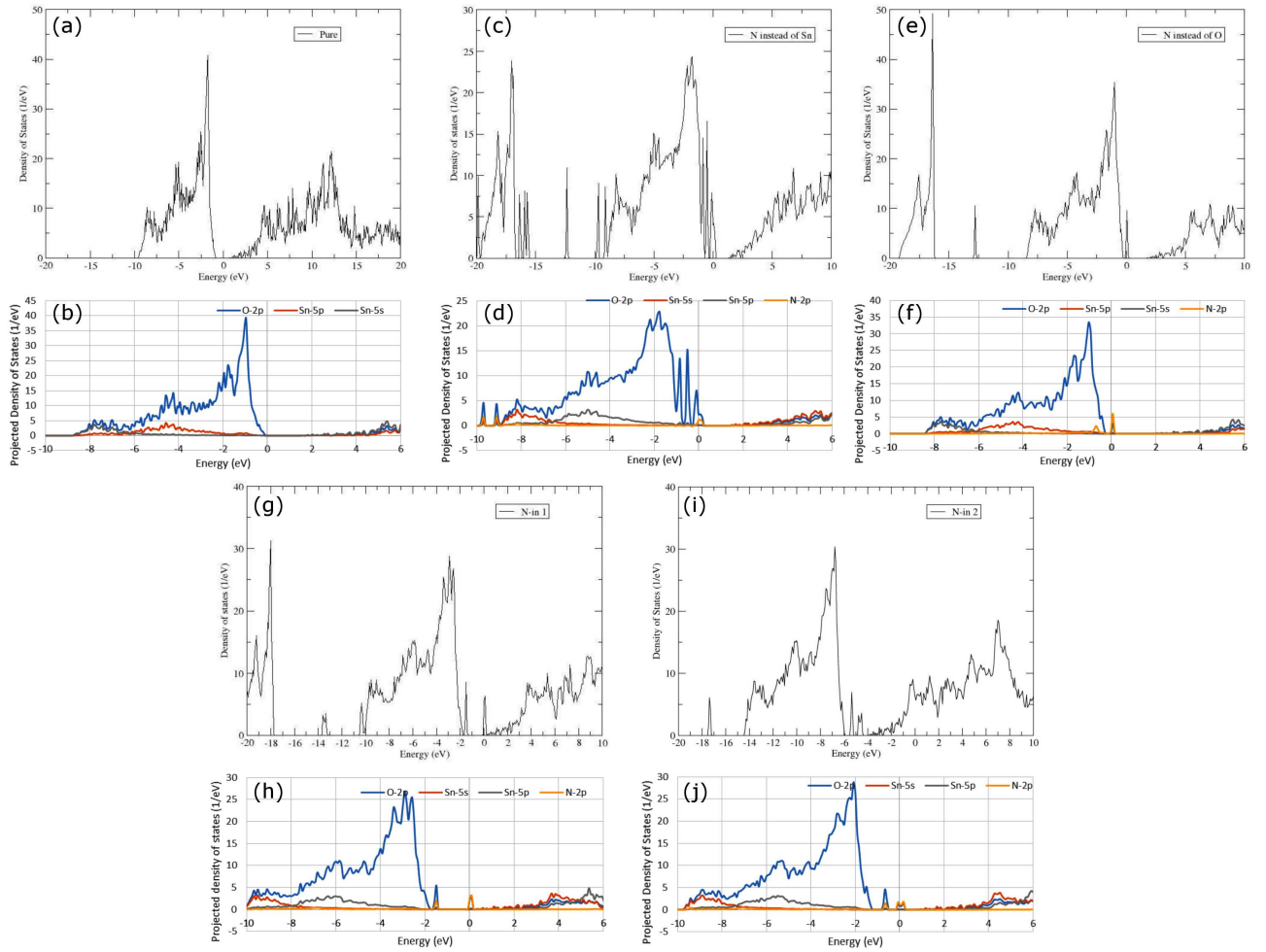


Fig. 4. Density of states and projected density of states of: (a, b) pure SnO_2 , (c, d) NSnO_2 — N instead of Sn, (e, f) NSnO_2 — N instead of O, (g, h) NSnO_2 — N-in-1, (i, j) NSnO_2 — N-in-2.

The band structure of pure SnO_2 and doped one in four different cases of substitutional and interstitial along the high symmetry directions of the Brillouin zone are evaluated, shown in Fig. 3. The band gap in pure case is about 2.1 eV at highly symmetric Γ -point, which is less than the experimental value of 3.6 eV.

It is obvious that the band gap is generally underestimated using DFT [16]. The valence band maximum and the conduction band minimum place at the same Γ -point denote that the lowest band gap transition in the SnO_2 rutile is direct. This is also in agreement with the previous theoretical calculations [12]. The curvature of the conduction band at the Γ -point, as shown in Fig. 3, is less flat than that at the top of the valence band, meaning a lower effective mass of the electron than that of the hole in the SnO_2 host.

The density of states and projected density of states of pure tin oxide and nitrogen doped tin oxide substituted instead of O and N and two interstitial cases depicted in Fig. 4 indicate that N_{Sn} , N_{O} , and $\text{N}_{\text{in-2}}$ show *p*-type character, which are in accordance with

the theoretical publications by Sun et al. [17]. The upper contribution of the valence band, for undoped SnO_2 , mainly conclude the O-2*p* states with the little portion of Sn-5*p* states. The bottom part of the conduction band derives basically from Sn-5*s* and Sn-5*p* states while O-2*p* states also have a little existence [12]. Mainly, the N-2*p* states start to mix with the valence band edge of SnO_2 in three cases of N_{O} , N_{Sn} , and $\text{N}_{\text{in-2}}$ sites leading in an obvious splitting above Fermi level E_{F} . At the end it result in an obvious band gap narrowing in the N-doped supercell. For N doped SnO_2 , the major effects in the band structures are to make acceptor states and transferring the Fermi level towards the valence band maximum resulting in *p*-type conducting semiconductor. In addition, the Fermi level enters into the valence band in all cases of the N-doped SnO_2 substitution in N_{O} , N_{Sn} , and $\text{N}_{\text{in-2}}$ sites except $\text{N}_{\text{in-1}}$. In the case of $\text{N}_{\text{in-1}}$, N-2*p* states begin to mix with the conduction band edge of SnO_2 and the Fermi level towards the conduction band minimum introducing donor level into the band gap. So in the case of $\text{N}_{\text{in-1}}$, it shows *n*-type

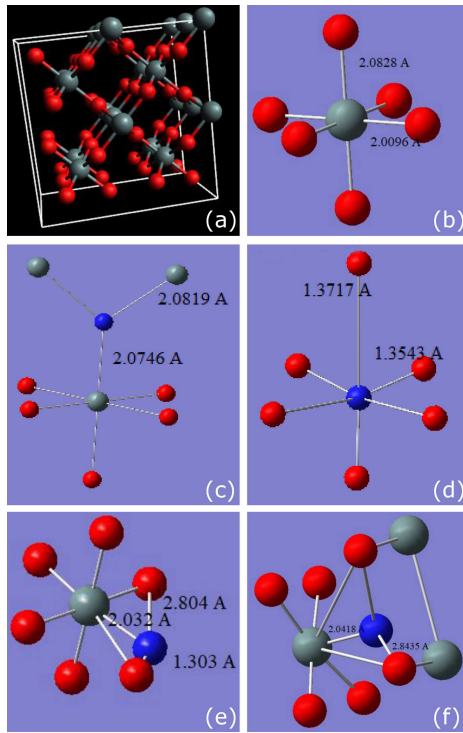


Fig. 5. (a) Supercell and partial geometry of pure and doped tin oxide: (b) pure SnO₂, (c) NSnO₂ — N instead of Sn, (d) NSnO₂ — N instead of O, (e) NSnO₂ — N_{in-1}, (f) NSnO₂ — N_{in-2} (Red balls are O, Gray balls are Sn, Blue balls are N).

conductivity. Any way the all optical band gap notably decreases in the N-doped SnO₂ system. The valence band enhances without changing of the conduction band, leading to the band gap reduction and then to the red-shift of photoluminescence (PL) [18–20].

The optimized 48 atom SnO₂ supercell is shown in Fig. 5. In the case of N_O, the optimal bond length of the N atom and adjacent Sn atom is 2.0819 Å and 2.0746 Å, respectively. Each of these bond lengths relaxes outward in comparison with the Sn-O bond length of 2.0828 Å and 2.0096 Å. This effect is caused by the N atomic radius which is slightly larger than that of O [17]. In the structure of N_{Sn}, the optimal N-O bond length is 1.3717 Å and 1.3543 Å, however its values relaxes inward of the Sn-O bond length 2.0096 Å and 2.0828 Å. It is due to N atomic radius which is so smaller than Sn atomic radius. The cases of N interstitial 1 and 2 correspond to the center of the two neighboring O atoms but in different locations. Differences in bond length was shown in the picture.

4. Conclusions

In this paper we have studied the effect of Nitrogen doping on tin oxide by fully self-consistent pseudopotential DFT method, when N was put in positions of Sn, O, and in two interstitial cases. In comparison with undoped

tin oxide, the band gap of doped tin oxide were reduced. The diagram of DOS and PDOS showed that substitution with N instead of Sn and O and N-in 2, lead to *p*-type conductivity, while the interstitial case of N-in 1 showed *n*-type conductivity.

Acknowledgments

This project was supported by the Islamic Azad University, Fouman and Shaft branch, Iran and performed in the Physics Department of the University of Guilan.

The author appreciates the friendly helps of Dr. Sepahi in this project.

References

- [1] K.G. Godinho, A. Walsh, G.W. Watson, *J. Phys. Chem. C* **113**, 439 (2009).
- [2] E. Albanese, C. Di Valentin, G. Pacchioni, F. Sauvage, *J. Phys. Chem. C* **119** 48 (2015).
- [3] T. Wang, H. Zhang, L. Tian, Y. Li, Y. Zhang, S. Cui, Y. Ding, J. Tang, R. Zhang, *Chem. Eng. Trans.* **51**, 1285 (2016).
- [4] A.M. Mudarra Navarro, C.E. Rodríguez Torres, A.F. Cabrera, M. Weissmann, K. Nomura, L.A. Errico, *J. Phys. Chem. C* **119**, 5596 (2015).
- [5] G. Zhang, G. Qin, G. Yu, Q. Hu, H. Fu, C. Shao, *Thin Solid Films* **520** 5965 (2012).
- [6] A. Fakhim Lamrani, M. Belaiche, A. Benyoussef, E. Kenz, *J. Appl. Phys.* **115**, 013910 (2014).
- [7] M. Batzill, U. Diebold, *Prog. Surf. Sci.* **79**, 47 (2005).
- [8] S.S. Pan, Y.X. Zhang, X.M. Teng, G.H. Li, L. Li, *J. Appl. Phys.* **103**, 093103 (2008).
- [9] J.B. Varley, A. Janotti, C.G. Van de Walle, *Phys. Rev. B* **81**, 245216 (2010).
- [10] S.S. Pan, G.H. Li, L.B. Wang, Y.D. Shen, Y. Wang, T. Mei, X. Hu, *Appl. Phys. Lett.* **95**, 222112 (2009).
- [11] S.S. Pan, C. Ye, X.M. Teng, X.M. Fan, G.H. Li, *Appl. Phys. A* (2006).
- [12] A. Slassi, *Opt. Quantum Electron.* **48**, 160 (2016).
- [13] J.M. Soler, E. Artacho, J.D. Gale, A. Garcia, J. Junquera, P. Ordejon, D. Sanchez-Portal, *J. Phys. Condens. Matter* **14**, 2745 (2002).
- [14] C. Freysoldt, et al., *Rev. Mod. Phys.* **86**, 253 (2014).
- [15] G. Rahman, N. Ud Din, *Phys. Rev. B* **87**, 205205 (2013).
- [16] A.M. Mazzone, V. Morandi *Comput. Mater. Sci.* **38**, 814 (2007).
- [17] X. Sun, R. Long, X. Cheng, X. Zhao, Y. Dai, B. Huang, *J. Phys. Chem. C* **112**, 9861 (2008).
- [18] D.X. Xing, P.J. Wang, C.W. Zhang, *4th Annu. Int. Conf. Mater. Sci. Eng.* 0554 (2016)(ICMSE 2016).
- [19] R. Long, N.J. English, *Phys. Lett. A* **374**, 319 (2009).
- [20] S. Guipeng, Y. Jinliang, N. Peijiang, M. Delan, *J. Semicond.* **37**, 023005 (2016).